Published in final edited form as:

Nat Methods. 2009 March ; 6(3): 215–218. doi:10.1038/nmeth.1300.

Nanomole-scale Protein Solid-state NMR by Breaking Intrinsic ^{1}H-T_1 Boundaries

Nalinda P. Wickramasinghe[1,#], **Sudhakar Parthasarathy**[1], **Christopher R. Jones**[1], **Chhavi Bhardwaj**[1], **Fei Long**[1], **Mrignayani Kotecha**[1], **Shahila Mehboob**[2], **Leslie W.-M Fung**[1], **Jaan Past**[3], **Ago Samoson**[3,4], and **Yoshitaka Ishii**[1]

[1] Department of Chemistry, University of Illinois at Chicago, 845 West Taylor Street, Chicago IL 60607, USA

[2] College of Pharmacy, University of Illinois at Chicago, 900 South Ashland Avenue, Chicago, IL 60607 USA

[3] National Institute of Chemical Physics and Biophysics, Akadeemia tee 23, 12618 Tallinn, Estonia

[4] Department of Physics, University of Warwick, Coventry, United Kingdom CV4 7AL

Abstract

We present an approach that speeds up protein solid-state NMR (SSNMR) by 5–20 fold by using paramagnetic doping to condense data-collection time (to ~0.2 s/scan), overcoming a long-standing limitation on slow recycling due to intrinsic ^{1}H T_1 longitudinal spin relaxation. By employing low-power schemes under magic-angle spinning at 40 kHz, we show that two-dimensional ^{13}C/^{13}C and ^{13}C/^{15}N SSNMR spectra can be attained for several to tens of nano-moles of β-amyloid fibrils and ubiquitin in just 1–2 days.

SSNMR is a versatile technology for the characterization of heterogeneous solids in the fields of chemistry, biology, and medicine.1–8 However, because of the restricted sensitivity of SSNMR, typically as much as 0.5–1 μmol samples are required for basic multi-dimensional SSNMR, which limits biological applications. Developments of new methodologies and hardware continue to address the sensitivity issues in NMR spectroscopy.1,9–11 For example, the introduction of Fourier-transform NMR in data acquisition drastically reduced the time requirement, compared to continuous-wave NMR.1

Correspondence to: Yoshitaka Ishii.

[#]The present address: Department of Biochemistry, Case Western Reserve University, 10900 Euclid Avenue, Cleveland, OH 44106, USA, E-mail: yishii@uic.edu, Phone: 312-413-0076, Fax: 312-996-0431

AUTHOR CONTRIBUTIONS

N.P.W. and Y.I. designed the experiments. N.P.W., S.P., C.R.J., C.B., F.L., M.K., and Y.I. performed the experiments. J. P. and A.S. constructed the NMR probe. F.L., S.M., and L.W.-M.F. established the expression system of α-spectrin II. N.P.W. and Y.I. wrote the paper.

Solid-state NMR spectroscopy is used to elucidate structural details about proteins which cannot be easily studied by x-ray crystallography, but because the technique is not very sensitive, large sample amounts are required, limiting its biological application. A combination of optimizations now increases the sensitivity of solid-state NMR spectroscopy by 5–20-fold.

Nevertheless, data collection for SSNMR has been generally inefficient due to long idling delays required for magnetization recovery between scans. Even in modern multi-dimensional SSNMR schemes designed for biomolecules,2–8 recycle delays typically consume 95–99 % of the experimental time. Despite the vast inefficiency, slow recycling (typically 1–4 s/scan) has been required in ^{13}C SSNMR to retrieve ^{1}H spin polarization for the cross polarization (CP) method during three times the ^{1}H longitudinal-relaxation time (T_1),1 which we call the "intrinsic ^{1}H T_1 boundary". For hydrated proteins ^{1}H T_1 may be shorter, yet recycle delays longer than $3T_1$ (2–4 s) are often needed to avoid sample heating by radio-frequency field (rf) irradiation.

Here, we propose an approach to break the long-standing ^{1}H T_1 boundary for hydrated proteins by combining paramagnetic doping,12 very-fast magic-angle spinning (MAS),10,13 and fast recycling of low-rf-power sequences.10,13 In this approach, which we call "paramagnetic-relaxation-assisted condensed data collection" (PACC), we achieved a reduction in ^{1}H T_1 by orders of magnitude down to 50–100 ms by carefully adjusting paramagnetic doping. In conventional SSNMR, paramagnetic doping is used to reduce long delays to a standard range (1–4 s) for systems with excessively long intrinsic ^{1}H T_1, including proteins.2,12,14 However, the possibility of such radical T_1 reduction and fast recycling required for PACC has not been previously examined particularly for multi-dimensional SSNMR, where long-term sample integrity should be retained despite possible heating due to fast recycling and line broadening due to paramagnetic dopants should be minimized. Here, we achieve very fast recycling (~0.2 s/scan) for hydrated proteins with PACC, accelerating data collection by 5–20 fold. This allowed us to analyze much smaller samples (several nano-moles) of ^{13}C- and ^{15}N-labeled proteins by 2D ^{13}C/^{15}N SSNMR.

First, we compared 2D ^{13}C/^{13}C chemical shift correlation SSNMR spectra (Fig. 1a) in the aliphatic regions for hydrated microcrystals of uniformly ^{13}C-labeled ubiquitin alone or in the presence of a Cu(II)-EDTA dopant (Supplementary Methods online). We obtained highly resolved spectra despite the moderate field strength (^{1}H NMR frequency 400 MHz) by applying a low-power 2D finite-pulse-rf-driven-recoupling (fpRFDR) ^{13}C/^{13}C-correlation sequence, which minimizes sample heating (Supplementary Fig. 1 online). Throughout this study, we applied spinning at 40 kHz for optimum decoupling performance by low-power two-pulse-phase-modulation (TPPM) decoupling. We set the recycle delays to three times the ^{1}H T_1 values; Cu(II) shortened ^{1}H T_1 of ubiquitin to 50 ms in the doped sample from 230 ms in the undoped sample via paramagnetic relaxation enhancement (PRE). Naturally, the recycle delay was notably reduced by doping. The PACC experiment took only 5.4 h (1.8 mg or ~200 nmol ubiquitin), while the standard experiment took 21.9 h. The superimposed 2D spectra (Fig. 1a) and the slices (Fig. 1b) show both the doped and undoped samples yield almost identical spectral intensities and chemical shifts (see also Supplementary Fig. 2 online). Therefore, information on conformations and structural disorders based on chemical shifts2–7 can be safely elucidated in the PACC approach. Despite the relatively short intrinsic ^{1}H T_1 of the undoped sample, the experimental time was still reduced by 4 fold; use of the low-power sequences allowed us to reduce the recycle delays by 3–5 fold to the optimum value (~0.7 s) from typical delays under high-power ^{1}H

decoupling (2–4 s). Therefore, our approach accelerated the 2D experiment by 12–20 fold for ubiquitin, compared with traditional experiments.

Figure 1c depicts a proposed relaxation-enhancement mechanism for hydrated proteins in micro-crystals doped with Cu-EDTA. Since protein micro-crystals typically contain a considerable amount of water (~33 % in volume for ubiquitin), Cu-EDTA dopants are likely to reach the protein surface by diffusion, relaxing ^{1}H near the surface. Because ^{1}H T_1 values for the protein were found to be homogeneous, ^{1}H magnetization retrieved by PRE is likely to be transferred to ^{1}H spins inside the protein via a “spin diffusion” mechanism. We confirmed this mechanism by experimental and theoretical analysis and we also tested the effects of other dopants, for cases when Cu-EDTA is not suitable (Supplementary Data and Supplementary Figs. 3–5 online). Our preliminary theoretical analysis, which reasonably agrees with experiments (Supplementary Table 1 online), suggests that for larger proteins the relaxation mechanism is less efficient. In such a case, the Cu-EDTA concentration can be adjusted as will be discussed below.

Next, we experimentally validated the applicability of PACC for larger systems using amyloid fibrils of Aβ(1–40) peptide associated with Alzheimer’s disease as an example.6,7 Amyloid proteins generally self-assemble into long insoluble fibrils of several nano-meters in diameter6–8 (see Supplementary Fig. 6 online for details about the sample used here). Their hydrophobic nature and large size (MW > 1 MDa) may limit the access of the dopants inside the fibrils. We found that the Cu-EDTA concentration required for PRE needed to be adjusted. A higher concentration of Cu-EDTA was necessary to reduce the ^{1}H T_1 to 77 ms, which is still longer than that for ubiquitin, but 7.3 times shorter than that of the undoped Aβ (560 ms). The recycle delays were set to three times the ^{1}H T_1 values (240 ms and 1.70 s). The PRE on ^{1}H T_1 shows reasonable agreement with our theoretical predictions (Supplementary Table 1 online), which indicate the PRE for the Aβ fibril is equivalent to that of a 70-kDa globular protein.

We superimposed the 2D ^{13}C/^{13}C correlation spectra (Fig. 1d) obtained for the fibril samples alone or in the presence of Cu-EDTA, for Aβ(1–40) (~1.4 mg) labeled with uniformly ^{13}C and ^{15}N-labeled amino-acids at Ala-30, Ile-32, Gly-38 and Val-39 for comparison. We obtained a 2D spectrum by PACC in only 3.1 h, in contrast to 20.5 h required for the standard approach. All the one-bond cross peaks were observed, except for Gly-38, for which signals were weak in both spectra presumably due to mobility. Comparison of these two spectra demonstrates that the paramagnetic doping induced no substantial changes in the line position or widths beyond the experimental error of ±0.2 ppm. Hence, the PACC approach is likely to be applicable for studying the structure of various amyloid fibrils and larger globular proteins.

In many cases, SSNMR analyses of biologically important systems are prohibited by difficulties in preparing isotope-labeled samples in large quantities (0.5–1 μmol). To demonstrate the application of PACC to mass-limited biological systems, we show a 2D ^{13}C/^{13}C correlation SSNMR spectrum of uniformly ^{13}C-and ^{15}N-labeled 42-residue Aβ(1–42) in fibrils (Fig. 2a). Although Aβ(1–42) is considered to be the most pathogenic Aβ species, previous SSNMR studies mostly focused on less aggregative Aβ(1–40)6,7 because

of the difficulties in sample preparation for Aβ(1–42). With the enhanced sensitivity of PACC, using only 87 nmol (0.4 mg) of the sample, we obtained a 2D SSNMR spectrum for uniformly ^{13}C-labeled Aβ(1–42) fibrils in 40 h. Overall, the signals show sharp lines (0.6–1.5 ppm), suggesting the presence of well ordered structures in the Aβ(1–42) fibrils. Various cross peaks between $^{13}C_{\alpha}$ and $^{13}C_{\beta}$, which are assigned to amino-acid types (circles in Fig. 2a), indicate a largely β-sheet structure for Ala, Val, Ile, and Leu residues.

2D ^{13}C/^{15}N correlation experiments are widely used as a building block of 3D/4D triple-resonance SSNMR. Although the intrinsically heterogeneous Aβ fibrils exhibit only modest resolution in ^{15}N chemical shifts, for biomolecules of higher structural regularity, including some amyloid fibrils and membrane proteins,3,5,8 2D ^{13}C/^{15}N experiments offer excellent resolution with higher sensitivity because of higher transfer efficiency between ^{13}C and ^{15}N pairs (~40 %; cf. ~10 % for ^{13}C-^{13}C transfer in Fig. 1a). Figure 2b shows a 2D ^{13}C/^{15}N correlation spectrum obtained for 22 nmol (200 μg) of uniformly ^{13}C- and ^{15}N-labeled ubiquitin microcrystals doped with 10 mM Cu-EDTA. Despite the limited sample quantity, a 2D spectrum with excellent resolution was obtained within 2.7 h by PACC (see Supplementary Fig. 7 online for comparison with the undoped sample). These results suggest that the PACC approach opens an avenue to attain 2D SSNMR of as little as 7 nmol of the protein in 22 h, which has not been obtained even by microcoil SSNMR.11

Unlike ^{1}H spins, spin diffusion of ^{13}C spins is much slower under fast MAS. Thus, lastly, we discuss the possibility of elucidating supramolecular structural information or solvent accessibility of biomolecules at site-specific resolution by examining PRE on ^{13}C T_1 relaxation rates ($R_1 \equiv 1/T_1$) for the Aβ(1–40) fibrils. We summarize the difference of ^{13}C R_1 in the presence and absence of Cu-EDTA (ΔR_1) (Fig. 3) for ^{13}C at different residues in Aβ(1–40). Clearly, ΔR_1 is highest for the N-terminal residues, which are known to be unstructured and thus should be more accessible to solvents.6 Aβ(1–40) in fibrils is expected to form two β-strands,6 one by the residues 10–22 and the other by the residues 30–40 (Fig. 3 inset). Our data show that ^{13}C in the two β-sheet regions, in particular $^{13}C_{\alpha}$ groups, have much smaller ΔR_1 than those for the N-terminal residues. This suggests that solvent accessibility to the β-sheet regions is restricted. As previously discussed,13 in rigid paramagnetic solids, ΔR_1 is proportional to $1/r^6$, where r is the distance between the paramagnetic ion and ^{13}C. Although a more detailed analysis is needed for quantitative interpretation, this suggests that evaluating supramolecular structures and solvent accessibility by PRE on ^{13}C R_1 for amyloid fibrils and other nano-structured proteins should be possible. In contrast to the previously demonstrated approach using ^{13}C R_2 PRE,15 long intrinsic ^{13}C T_1 (~s) can be modulated at lower doping level without affecting resolution. Thus, the doped sample prepared for the ^{13}C R_1 PRE measurements can be used for other multi-dimensional experiments with enhanced sensitivity.

Unlike other methods for enhancing the sensitivity of SSNMR, our approach does not impose any major restrictions on an arsenal of NMR experiments. With further development, this PACC approach could accelerate a variety of standard biomolecular SSNMR experiments for amyloid fibrils and other systems such as cytoskeletal proteins (Supplementary Fig. 8 online) and possibly paramagnetic proteins.16 Although the slow ^{1}H spin diffusion may limit the sensitivity advantage for a larger globular protein having a

diameter of > 7 nm (MW > 100 kDa; see Supplementary Data online), the PACC approach is likely to be applicable to other classes of important systems having nano-meter dimensions. Our experiments also suggest that the PACC approach will allow for efficient multi-dimensional SSNMR structural analysis for various biomolecules on a nano-mole scale. This will markedly reduce the need for preparing samples in large quantities. In SSNMR experiments with membrane proteins, the proteins usually constitute only a minor fraction of the sample.4,5 Thus, it is encouraging that a reasonable quality of 2D $^{13}C/^{15}N$ correlation was obtained in 3 h for ubiquitin occupying only 2% (200 nL) of the allowed sample volume (10 μL) in a rotor. Finally, our preliminary ^{13}C T_1 analysis for Aβ peptides suggests the possibility of examining supramolecular structures or solvent accessibility in amyloid fibrils by site selective modulation of ^{13}C relaxation rates. The PACC approach should provide access to structural features that are difficult to obtain by other methods.

Supplementary Material

Refer to Web version on PubMed Central for supplementary material.

Acknowledgments

This work was supported in part by the Dreyfus Foundation Teacher-Scholar Award program, the NSF CAREER program (CHE 449952), Alzheimer's Association IIRG grant (08-91256), and the NIH RO1 program (AG028490) for YI, and Estonian Science foundation programs for AS. We are grateful to Dr. Robert Tycko at the NIH for providing a structural model6 used for Fig. 3.

References

1. Ernst, RR.; Bodenhausen, G.; Wokaun, A. Principles of nuclear magnetic resonance in one and two dimensions. Oxford University Press; Oxford: 1987. p. 146
2. Weliky DP, Bennett AE, Zvi A, Anglister J, Steinbach PJ, Tycko R. Solid-state NMR evidence for an antibody-dependent conformation of the V3 loop of HIV-1 gp120. Nat Struct Biol. 1999; 6:141–145. [PubMed: 10048925]
3. Igumenova TI, McDermott AE, Zilm KW, Martin RW, Paulson EK, Wand AJ. Assignments of carbon NMR resonances for microcrystalline ubiquitin. J Am Chem Soc. 2004; 126:6720–6727. [PubMed: 15161300]
4. Mani R, Cady SD, Tang M, Waring AJ, Lehrert RI, Hong M. Membrane-dependent oligomeric structure and pore formation of beta-hairpin antimicrobial peptide in lipid bilayers from solid-state NMR. Proc Natl Acad Sci U S A. 2006; 103:16242–16247. [PubMed: 17060626]
5. Lange A, Giller K, Hornig S, Martin-Eauclaire MF, Pongs O, Becker S, Baldus M. Toxin-induced conformational changes in a potassium channel revealed by solid-state NMR. Nature. 2006; 440:959–962. [PubMed: 16612389]
6. Petkova AT, Yau WM, Tycko R. Experimental constraints on quaternary structure in Alzheimer's beta-amyloid fibrils. Biochemistry. 2006; 45:498–512. [PubMed: 16401079]
7. Chimon S, Shaibat MA, Jones CR, Calero DC, Aizezi B, Ishii Y. Evidence of fibril-like β-sheet structures in neurotoxic amyloid intermediate for Alzheimer's β-amyloid. Nat Struct Mol Biol. 2007; 14:1157–1164. [PubMed: 18059284]
8. Wasmer C, Lange A, Van Melckebeke H, Siemer AB, Riek R, Meier BH. Amyloid fibrils of the HET-s(218–289) prion form a beta solenoid with a triangular hydrophobic core. Science. 2008; 319:1523–1526. [PubMed: 18339938]
9. Hall DA, Maus DC, Gerfen GJ, Inati SJ, Becerra LR, Dahlquist FW, Griffin RG. Polarization-enhanced NMR spectroscopy of biomolecules in frozen solution. Science. 1997; 276:930–932. [PubMed: 9139651]

10. Ishii Y, Yesinowski JP, Tycko R. Sensitivity enhancement in solid-state C-13 NMR of synthetic polymers and biopolymers by H-1 NMR detection with high-speed magic angle spinning. J Am Chem Soc. 2001; 123:2921–2922. [PubMed: 11456995]
11. Edison AS, Long JR. Spectroscopy - The magic of solenoids. Nature. 2007; 447:646–647. [PubMed: 17554293]
12. Ganapathy S, Naito A, McDowell CA. Paramagnetic doping as an aid in obtaining high-resolution 13C NMR spectra of biomolecules in solid-state. J Am Chem Soc. 1981; 103:6011–6015.
13. Wickramasinghe NP, Shaibat M, Casabianca LB, de Dios AC, Harwood JS, Ishii Y. Progress in 13C and 1H solid-state NMR for paramagnetic systems under very fast MAS. J Chem Phys. 2008; 128:52210.
14. Linser R, Chevelkov V, Diehl A, Reif B. Sensitivity enhancement using paramagnetic relaxation in MAS solid-state NMR of perdeuterated proteins. J Magn Reson. 2007; 189:209–216. [PubMed: 17923428]
15. Buffy JJ, Hong T, Yamaguchi S, Waring AJ, Lehrer RI, Hong M. Solid-state NMR investigation of the depth of insertion of protegrin-1 in lipid bilayers using paramagnetic Mn2+ Biophys J. 2003; 85:2363–2373. [PubMed: 14507700]
16. Pintacuda G, Giraud N, Picrattelli R, Bockmann A, Bertini I, Emsley L. Solid-state NMR spectroscopy of a paramagnetic protein: Assignment and study of human dimeric oxidized Cu-II-Zn-II superoxide dismutase (SOD). Angew Chem Int Edit. 2007; 46:1079–1082.

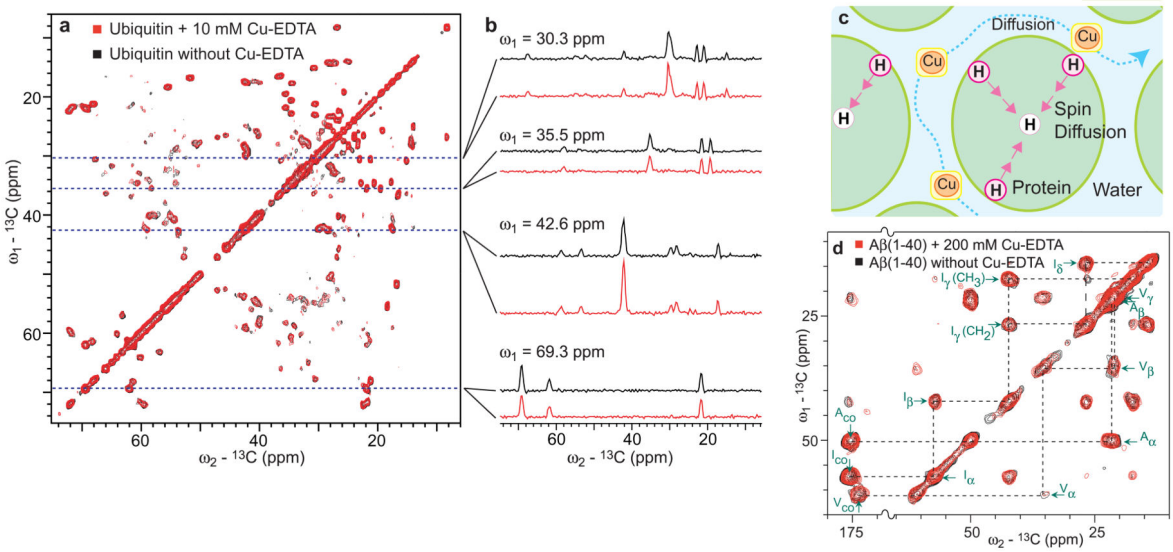

Figure 1.

The effectiveness of the PACC approach for hydrated proteins. (**a**) Comparison of superimposed 2D $^{13}C/^{13}C$ chemical-shift correlation SSNMR spectra of uniformly ^{13}C-labeled ubiquitin (1.8 mg) in microcrystals in the (black) absence and (red) presence of 10 mM Cu(II)-EDTA respectively obtained in standard and PACC approaches at a ^{1}H frequency of 400.2 MHz, together with (**b**) slices at selected positions. (**c**) A proposed mechanism of paramagnetic ^{1}H T_1 relaxation enhancement for hydrated protein microcrystals by Cu(II)-EDTA doping. (**d**) Comparison of 2D $^{13}C/^{13}C$ SSNMR spectra of fibrillized ^{13}C- and ^{15}N-labeled 40-residue Alzheimer's β-amyloid (Aβ(1–40); 1.4 mg) that were obtained in the (red) presence and (black) absence of 200 mM Cu-EDTA. All the experiments in Fig. 1 were performed at a spinning speed of 40 kHz with signal acquisitions under low-power TPPM decoupling at rf-fields of 7 kHz. The mixing time for the fpRFDR sequence was 1.6 ms. See Supplementary Methods and Supplementary Figs. 1, 2, 6 online for sample preparations, signal assignments for ubiquitin, pulse sequences, and other details.

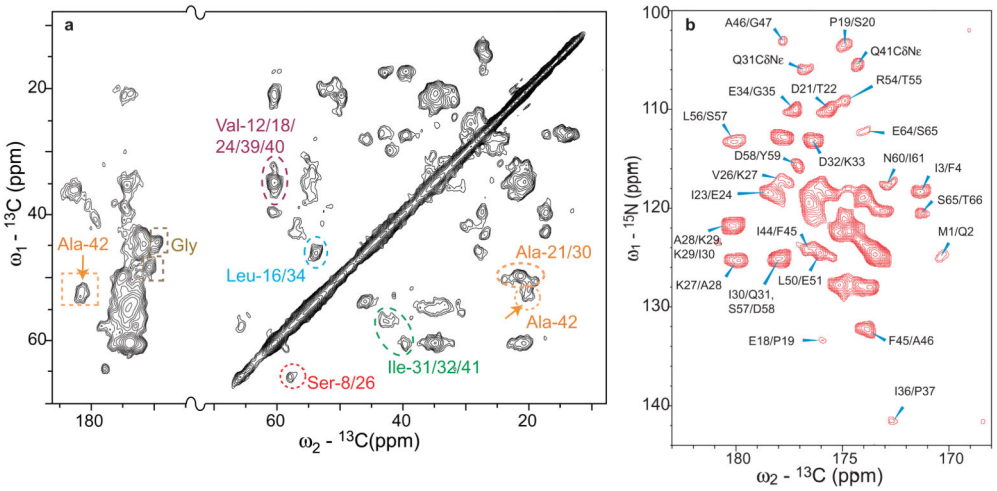

Figure 2.

2D chemical-shift correlation SSNMR spectra for mass-limited systems by the PACC approach. **(a)** A 2D $^{13}C/^{13}C$ correlation SSNMR spectrum obtained by PACC for fibrillized uniformly ^{13}C- and ^{15}N-labeled 42-residue Alzheimer's β-amyloid (Aβ) peptide (0.4 mg or 80 nmol) doped with 200 mM Cu-EDTA, together with preliminary assignments based on amino-acid types for $^{13}C_\alpha/^{13}C_\beta$ cross peaks (dotted circles) and $^{13}C_\alpha/^{13}CO$ (dotted squares). The recycle delays were set to 180 ms, which is approximately three times the ^1H T_1 value (~ 60 ms). The presence of strong cross peaks for Ala-42 (orange arrows) suggest the ordered structure at the C-terminal of Aβ(1–42). **(b)** Nano-mole scale analysis by 2D $^{13}CO/^{15}N$ correlation SSNMR of uniformly ^{13}C- and ^{15}N-labeled ubiquitin (22 nmol or 200 μg) in microcrystals doped with 10 mM Cu-EDTA. The experimental time was only 2.7 h with recycle delays of 165 ms (^1H T_1 ~ 55 ms). After the first cross-polarization, ^{15}N signals were observed during the t_1 period (t_1^{max} = 12 ms) under low-power TPPM decoupling sequence. The real or imaginary component of the signal was transferred to ^{13}CO by double-quantum ^{13}C-^{15}N ramped cross polarization, in which the rf-intensity for ^{13}C ($\omega_C/2\pi$) was swept from 27 to 23 kHz while that for ^{15}N ($\omega_N/2\pi$) was fixed at 15 kHz during the contact time of 5 ms. See the Supplementary Methods and Supplementary Fig. 1 online for further details about the pulse sequences and sample preparation.

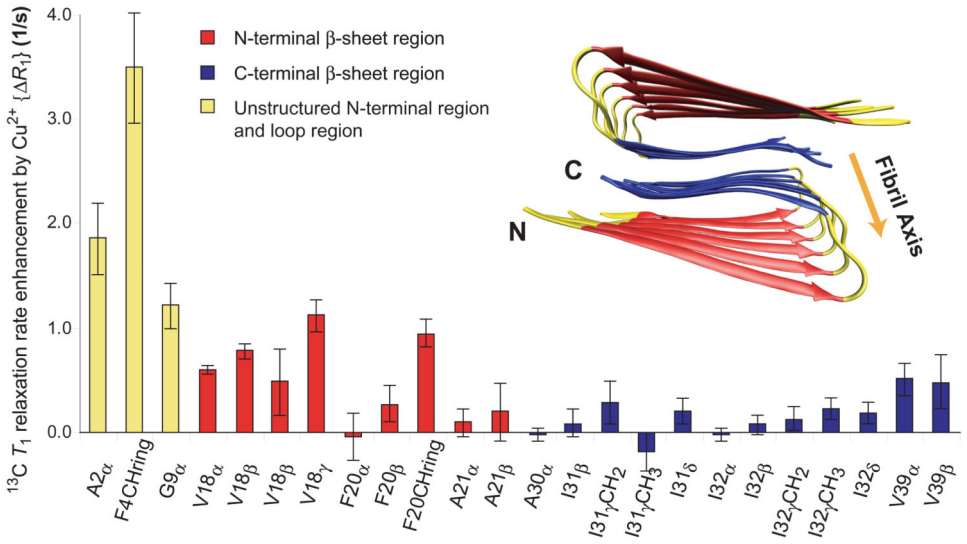

Figure 3.

^{13}C T_1 relaxation rate enhancement (ΔR_1) by 200 mM Cu-EDTA paramagnetic relaxation agent on Aβ(1–40) fibrils. The data were collected for three Aβ samples labeled with uniformly ^{13}C- and ^{15}N-labeled amino acids at selected sites in different schemes as (1) Ala-2, Phe-4, Gly-9, Val-18, (2) Val-18, Phe-20, Ala-21, Ile-31, Gly-33 and (3) Ala-30, Ile-32, Gly-38, Val-39. ^{13}C longitudinal relaxation rates R_1 were measured in the presence (R_1') and absence (R_1^{dia}) of Cu-EDTA by inversion recovery experiments detected in 1D ^{13}C CPMAS spectra at a spinning speed of 40 kHz at ^{1}H frequency of 400.2 MHz. ΔR_1 was obtained from $\Delta R_1 = R_1' - R_1^{dia}$. The color coding corresponds to the data for the unstructured N-terminal region (yellow: Residue 1–9), the N-terminal β-sheet region (red: Residue 10–22), and the C-terminal β-sheet region (blue: Residue 30–40).6 The structural model based on ref. 6 in the inset is also color coded as described above with the loop region (Residue 23–29), which is also denoted in yellow. See the Supplementary Methods online for further details about the experiments and the sample preparation.